ANGULAR ENERGY FLOW IN PERTURBATIVE QCD

I.I.Y. BIGI
CERN, Geneva, Switzerland

and

T.F. WALSH
Deutsches Elektronen-Synchrotron DESY, Hamburg, Germany

Received 15 December 1978

We discuss a general way in which QCD can be checked in lepton-induced reactions – even with low statistics data. This is the "angular energy flow", or the average energy fraction outside a cone of opening angle 2δ about the principal jet axis. in the final state of deep inelastic reactions. We illustrate this method by a perturbative calculation of the angular energy flow in $e^+e^- \to q\bar{q}g \to$ jets. This perturbative approach can be extended to other deep inelastic reactions with gluon jets. At high enough energy, it should test QCD beyond lowest order in α_s.

In field theories, it is likely that the final state of deep-inelastic processes (e^+e^--annihilation in particular) consists of multiple jets of particles [1–3]. Quantum chromodynamics (QCD) [4] is particularly important, as it is a candidate for the theory of the strong interactions. It probably even predicts [5] multiple jets at a small level – order $\alpha_s(Q^2)/\pi = [g_s(Q^2)]^2/4\pi \lesssim 0.1$, where $g_s(Q^2)$ is the effective coupling of the theory at distances $1/(Q^2)^{1/2}$ and $g_s^2(Q^2 = E^2) = 24\pi^2/[(33 - 2N_F) \ln (E/\Lambda)]$, N_F = number of flavors.

Given extensive data, it will be possible to carry out detailed tests of QCD in e^+e^--annihilation. Without this commodity it is necessary to devise something simpler. We propose studying the "angular energy flow" [6,7], the average fraction of the total hadronic energy (including neutrals) found outside a cone of full opening angle 2δ about the principal jet axis ‡1. (This might also work if only charged particle energy is counted.) We will show that this can be calculated perturbatively in QCD. It should also provide tests of QCD beyond leading order in α_s.

The lowest order QCD diagram giving multiple jets (three) [3], is shown in fig. 1a. The jets arise from fragmentation of the colored quarks or gluons into color singlet hadrons. These jets carry the energy of the parent quantum. At not too high energies the main effect of fig. 1 is to broaden the lowest order $e^+e^- \to q\bar{q} \to$ two jets by bremsstrahlung of a large $p_\perp$ gluon. We will calculate an energy-weighted cross section for two reasons. Firstly, by adding the energies of all particles in a jet we obtain the energy of the parent quantum ‡2. Thus we can compute fig. 1 directly without having to worry about how a q or g fragment into hadrons. Secondly, cross sections diverge as $[p_{\mathrm{gluon}} \times (1 - \cos\theta_{qg})]^{-1}$ when the gluon momentum is small or parallel to the momentum of the quark which radiated it. However, if one calculates energy-weighted quantities, there is no obvious $p_{\mathrm{gluon}} \to 0$ divergence. Of course, the angular singularity remains and forces us to introduce a cutoff in angle, $\delta_{\min}$. We will discuss later how to choose this cutoff angle.

‡1 The smallness of the short distance coupling in QCD means that there is a principal axis [8] for events in e^+e^--annihilation (and elsewhere). This axis is in general near (but not identical to) the "original" $q\bar{q}$ direction in $e^+e^- \to q\bar{q}$ [9]. We will use this principal axis in what follows.

‡2 We assume that the jet "mass" is small compared to its energy.

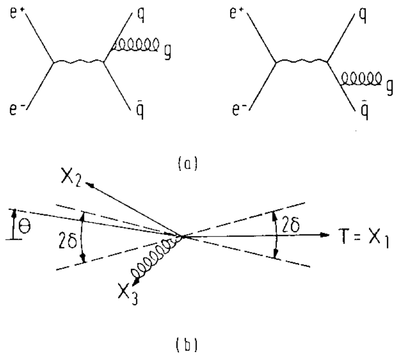

Fig. 1. (a) The perturbation diagrams for $e^+e^- \to q\bar{q}g$, and (b) the cone discussed in the text.

As principal axis we use the "thrust" [8,9] axis defined by ‡3

$$T_{\text{had}} = \max\left(\Sigma_i |\boldsymbol{p}_{\parallel}^i| / \Sigma_i |\boldsymbol{p}^i|\right) , \tag{1}$$

with our assumption, $T_{\text{had}} = T_{q\bar{q}g} = \max(x_1, x_2, x_3)$, $x_m = 2|\boldsymbol{p}_m|/E$, $E^2 = Q^2 = 4E_B^2$, where $1 = q$, $2 = \bar{q}$, $3 = g$. The cross section for $e^+e^- \to q\bar{q}g$ is well known [3]; we define an angle variable $\eta = \frac{1}{2}(1 + \cos\theta)$ (fig. 1b) and Born cross section $\sigma_0 = 3e_q^2 \sigma(e^+e^- \to \mu^+\mu^-)$ and find to order $\alpha_s(E) = 6\pi/[(33 - 2N_F)\ln(E/\Lambda)]$ the energy-weighted cross section ‡4

$$\frac{1}{E}\frac{dE}{d\eta\, dT} = \frac{1}{2}\sum_{n,(a),(b),(c)} x_n \frac{1}{\sigma_0}\frac{d\sigma_{q\bar{q}g}}{d\eta\, dT}$$
$$= \frac{1}{2}\frac{2\alpha_s(E)}{3\pi}\frac{T}{1-\eta T}\sum_{n,(a),(b),(c)} x_n^2 \frac{x_1^2 + x_2^2}{(1-x_1)(1-x_2)} , \tag{2}$$

where n runs over the gauge quanta opposite the one whose direction and magnitude defines T, $\eta \leqslant 1 - (\delta_{\min}/2)^2$ cuts out small $\theta < \delta_{\min}$ and a, b, c are:

(a) $x_1 = T$ for which

$$n = 2: \quad x_2 = \frac{1-T}{1-T\eta}, \quad x_3 = \frac{1-(2-T)T\eta}{1-T\eta};$$
$$n = 3: \quad x_2 = \frac{1-(2-T)T\eta}{1-T\eta}, \quad x_3 = \frac{1-T}{1-T\eta}; \tag{3a}$$

(b) $x_2 = T$ (analogous to (a));

(c) $x_3 = T$ for which

$$n = 1: \quad x_1 = \frac{1-T}{1-T\eta}, \quad x_2 = \frac{1-(2-T)T\eta}{1-T\eta},$$
$$n = 2: \quad x_1 = \frac{1-(2-T)T\eta}{1-T\eta}, \quad x_2 = \frac{1-T}{1-T\eta}. \tag{3b}$$

The kinematically allowed range of T is determined by η to be

$$1/2\eta \leqslant T \leqslant 1 , \qquad \text{if } \tfrac{1}{2} \leqslant \eta \leqslant \tfrac{3}{4} ,$$
$$[1 - (1-\eta)^{1/2}]/\eta \leqslant T \leqslant 1 , \quad \text{if } \tfrac{3}{4} \leqslant \eta .$$

We are principally interested in eq. (2) integrated over all T and over all $\frac{1}{2} \leqslant \eta \leqslant y = \frac{1}{2}(1 + \cos\delta)$ i.e., in the fraction of E outside the cone of full opening angle $2\delta > 2\delta_{\min}$. It is important to realize that eq. (2) only gives the energy between η and $\eta + d\eta$ per gauge quantum, and that there are kinematic correlations between the two quanta opposite the most energetic one. These must be taken into account when integrating eq. (2). For $\frac{1}{2} \leqslant \eta \leqslant \frac{3}{4}$ only one quantum at a time can lie outside the cone. For $\frac{3}{4} \leqslant \eta \leqslant 1 - (\delta_{\min}/2)^2$ either one or two quanta can lie outside 2δ. For $2 - 1/\eta \leqslant T \leqslant 1$ only one quantum is outside, and for $[1 - (1-\eta)^{1/2}]/\eta \leqslant T \leqslant 2 - 1/\eta$, two are. This has to be taken into account when weighting the energy outside the cone. Then we have

$$F_{\text{QCD}}(E, \delta) = \int_{1/2}^{y} d\eta \int_{T_{\min}}^{1} dT \frac{1}{E}\frac{dE}{d\eta\, dT} . \tag{4}$$

We computed eq. (4) numerically for $E = 30$ GeV, setting $\alpha_s = (30\text{ GeV}) = 0.200$ for the parameter $\Lambda = 0.5$ GeV and $N_F = 5$. The result is shown in fig. 2. (For comparison we also present $F_{\text{np}}(E, \delta)$ for a model with finite-$p_\perp$ quark jets only ‡5.) We have also carried out the perturbation calculation for the case of scalar gluons. The shape of $F(E, \delta)$ does not change significantly. Taking the charm quark mass into account also does not affect

‡3 $\boldsymbol{p}_{\parallel}$ is defined relative to an axis and the T axis itself is the one maximizing $\Sigma|\boldsymbol{p}_{\parallel}|$.

‡4 Note that this is not the quantity originally calculated by Sterman and Weinberg [2]. An energy-weighted correlation has recently been calculated by Basham et al. [10].

‡5 This model assumes that all quarks in $e^+e^- \to q\bar{q}$ fragment as $z\, dN/dz\, dp_\perp^2 \sim (1-z)^2 \exp(-bp_\perp^2)$ with $b^{-1} = 0.15\text{ GeV}^2$. The angular energy flow is just the integral of $z\, dN/dz\, dp_\perp^2$ and is unity for $\delta = 0$ (all energy outside the cone). It drops rapidly away from $\delta = 0$, falling at high energy as E^{-1} for fixed δ. (See also ref. [7].)

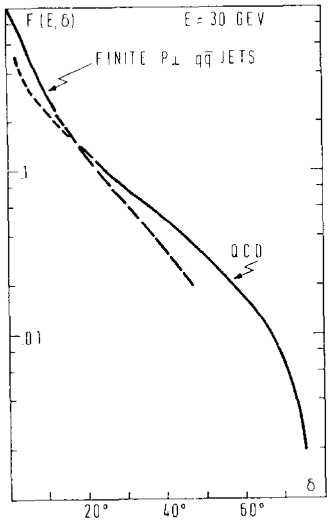

Fig. 2. The quantity $F_{QCD}(E, \delta)$ for E = 30 GeV and 5 flavors. Also shown is the expected (nonperturbative) $F_{np}(E, \delta)$ for a bounded $p_\perp$ jet at E = 30 GeV.

our results significantly at these energies (we have done this using the cross section quoted in ref. [11]).

In order to use our result at other energies, note that

$$F_{QCD}(E, \delta) = [\ln (E_0/\Lambda)/\ln (E/\Lambda)]\, F_{QCD}(E_0, \delta) . \quad (5)$$

(It is important to check the log E scaling behaviour of eq. (5); it is as much a prediction of QCD, as is the absolute magnitude of F.)

From fig. 2 we see that at E = 30 GeV, the QCD prediction for $F(E, \delta)$ dominates over the contribution of a finite-$p_\perp$ jet for $\delta > 20^\circ$. However, for the PLUTO data at E = 9.4 GeV, $F_{exp}(9.4, 60^\circ) \approx 0.15$ [6], whereas $F_{QCD} \approx 0.03$. Jets at this energy are much broader than the QCD expectation. Of course at fixed δ a finite-$p_\perp$ jet leads to $F_{np}(E, \delta)$ decreasing rapidly with E (F_{np} as E^{-1} in our finite-$p_\perp$ jet model). Thus we expect that as E increases, the experimental $F(E, \delta)$ will shrink rapidly down onto $F_{QCD}(E, \delta)$. Further shrinkage is only logarithmic, as expressed in eq. (5).

We expect that $F(E, \delta)$ will change significantly on passing the threshold for pair production of new quark flavors. Weak decays of new quarks lead to nearly isotropic events near threshold. Since light quark flavors do not populate $F(E, \delta)$ at large δ, the signature for a new threshold is a dramatic jump in $F(E, \delta)$ for large δ [‡6]. However, $F_{np}(E, \delta)$ arising from these nonperturbative new quark jets eventually drops as $1/E$

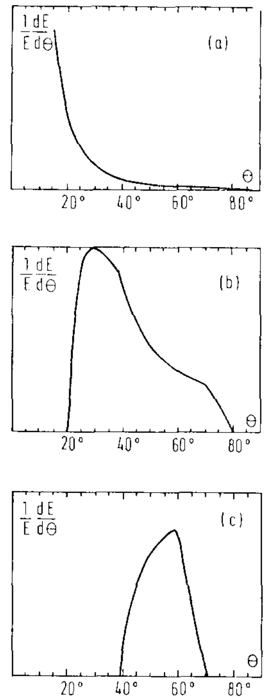

Fig. 3. $E^{-1}\, \mathrm{d}E/\mathrm{d}\theta$ for (a) $0.85 \leqslant T \leqslant 1$, (b) $0.75 \leqslant T \leqslant 0.85$, (c) $0.5 \leqslant T \leqslant 0.75$.

for large δ. Hence at high enough energies the perturbative QCD prediction again becomes relevant.

With more data than needed to check $F_{QCD}(E, \delta)$, one can look at a slightly more differential quantity, the "angular energy density" [6,7]

$$E^{-1}\, \mathrm{d}E/\mathrm{d}\cos\theta \, , \quad (6)$$

which can be obtained from eq. (2) by integration over T. In figs. 3a–c we show $E^{-1}\, \mathrm{d}E/\mathrm{d}\theta$ in various thrust bins at E = 30 GeV [‡7]. For T near unity there is a steep rise at small θ due to the angular singularity mentioned earlier. For comparison of the remaining plots with data, it is important to remember that the forward jet contributes asymptotically a term to $F(E, \delta)$ or expression (6) which is proportioanl to a delta function at zero angle. At finite E this is broad-

‡6 It is clear that $F(E, \delta)$ at large δ is even sensitive to new flavors of charge $-1/3$, which lead to a very small rise in $R = \sigma(e^+e^- \to \text{hadrons})/\sigma(\mu^+\mu^-)$ (cf. ref. [12]).

‡7 We follow ref. [6], where data are presented for $E^{-1}\, \mathrm{d}E/\mathrm{d}\theta$ in the thrust bins shown in figs. 3a–c.

ened by nonperturbative fragmentation effects. These disappear rapidly with increasing E. In fig. 3b there are three ranges of θ. The behavior at small and large θ is determined by phase space and the expanding integration range in T. At intermediate θ there is a "bite" in $E^{-1}\,\mathrm{d}E/\mathrm{d}\theta$, due to the fact that the kinematically allowed integration range in T for this bin does not change for this θ range. In this range one just sees a bremsstrahlung spectrum. At small T the allowed range in θ is sharply restricted by massless three-body kinematics. At high energies, data for this bin should show a sharp drop as θ increases away from small values $\theta < \delta_{\mathrm{min}}$ (where the forward peak is located) followed by the striking bump shown in fig. 3c.

It will be interesting to extend all this to the angular energy flow in deep inelastic lepton hadron reactions. One can also compare e^+e^- data for $F(E, \delta)$ directly to leptoproduction data. For this, one needs to choose a reference frame. The comparison of leptoproduction and e^+e^- is clearest in the Breit system [13] where $Q = p'_\ell - p_\ell = (0, Q)$ (p'_ℓ, p_ℓ are outgoing and incoming lepton momenta in $\ell N \to \ell' +$ jets). The hadron kinematics is collinear in this frame, the struck (recoil) quark having $p_{\mathrm{quark}} = -Q/2$ $(+Q/2)$. The construction of the cone analogous to that in fig. 1 is thus straightforward. It is, however, amusing to note that one can find a Lorentz frame in which the struck and recoil quark energies are fixed, although Q^2 can vary. (The orientation of struck and recoil quark three-momenta relative to one another varies with Q^2, of course.) This frame might be useful in looking for the QCD-induced quark and gluon substructure as the probe wavelength $1/(Q^2)^{1/2}$ varies at fixed quark energy. Of course, we do not expect $F(E, \delta)$ in deep-inelastic reactions to be affected much by production of new quark flavors (even charm). New flavors are produced only via the $Q\bar{Q}$ "sea" or (in neutrino reactions) by mixing with valence u and d quarks. Both effects are small.

We now discuss the range of validity in δ of $F(E, \delta)$. The expression (2) for the energy-weighted cross section shows an apparent singularity for $y = 1$. This is cancelled in perturbation theory by virtual corrections to $e^+e^- \to q\bar{q}$ [2]. But we can just as well evade it by introducing the cutoff $\theta > \delta_{\mathrm{min}}$, $\eta \leqslant 1 - (\delta_{\mathrm{min}}/2)^2$. Provided $\delta_{\mathrm{min}} > \delta_{\mathrm{np}}$ (the angle for non-perturbative $e^+e^- \to q\bar{q} \to$ two jets), fig. 1a can be used to calculate $F(E, \delta)$. We then expect that the criterion for F to be calculable by lowest order perturbation theory is simply that it be small compared to unity. For example,

$$F_{\mathrm{QCD}}(E, \delta_{\mathrm{min}}) = 0.3\,, \tag{7}$$

should provide an estimate of the minimum angle δ_{min}, for which eq. (2) is valid [‡8]. Numerically, we find

$$F_{\mathrm{QCD}}(30\,\mathrm{GeV}, 7.5^\circ) = F_{\mathrm{QCD}}(100\,\mathrm{GeV}, 4.2^\circ)$$
$$= F_{\mathrm{QCD}}(300\,\mathrm{GeV}, 2.5^\circ) = 0.3\,. \tag{8}$$

We can fix δ_{min} in an alternative way by considering only the leading logarithms in $F_{\mathrm{QCD}}(E, \delta)$. These will dominate eventually if $\delta_{\mathrm{min}} \to 0$. Calculation gives

$$F_{\mathrm{QCD}}(E, \delta) \underset{\delta \to 0}{\longrightarrow} (\alpha_s(E)/6\pi)(\ln \tfrac{1}{2}(1 - \cos\delta))^2\,, \tag{9}$$

and value (7) yields $F(E, \delta_{\mathrm{min}}) = 0.3 = 2\alpha_s(E) \times (\ln \delta_{\mathrm{min}}/2)^2/3\pi$ or

$$\delta_{\mathrm{min}} \sim 2\exp(-(0.45\,\pi/\alpha_s(E))^{1/2})\,, \tag{10}$$

or, for $E = 30$ GeV,

$$\delta_{\mathrm{min}} \sim 8^\circ\,.$$

Since the two values (7), (10) differ a bit, we have also considered non-leading logarithms. Including these gives

$$F_{\mathrm{QCD}}(E, \delta) \underset{\delta \to 0}{\longrightarrow} (\alpha_s(E)/3\pi)\{\tfrac{1}{2}(\ln \tfrac{1}{2}(1 - \cos\delta))^2$$
$$+ (\tfrac{15}{8} - 2\ln 2)\ln \tfrac{1}{2}(1 - \cos\delta)\}\,. \tag{11}$$

Remarkably enough, the leading term in eq. (11) is a good approximation to the exact result for $55^\circ \gtrsim \delta \gtrsim 10^\circ$; terms constant as $\delta \to 0$ seem even to cancel the non-leading log in eq. (11).

For $\delta < \delta_{\mathrm{min}}$ it is necessary to go beyond lowest order in calculating F_{QCD}. As we have indicated, this cannot be done for $\delta_{\mathrm{min}} \sim \delta_{\mathrm{np}}$ (i.e. $E \sim 30$ GeV), as confinement plays the essential role for $\delta < \delta_{\mathrm{np}}$. At high enough energies, we can hope that perturbation theory can be summed so as to yield $F_{\mathrm{QCD}}(E, \delta)$ for $\delta_{\mathrm{np}} < \delta < \delta_{\mathrm{min}}$. Then $F(E, \delta)$ can test QCD beyond leading order.

We gratefully acknowledge essential advice for our numerical calculations which was extended to us quite

[‡8] This is like the procedure used by Sterman and Weinberg [2].

readily by H. Krasemann and many other people, it was a delight to work in the DESY TSO terminal room where help was never far away. We are also indebted to Z. Kunszt for an informative conversation. One of the authors (I.B.) also wants to thank the theory group at DESY, where this work was finished, and the theory group at Rutherford Laboratory, where it was started, for their kind hospitality.

References

[1] A.M. Polyakov, JETP 32 (1971) 296; 33 (1971) 850.
[2] G. Sterman, Illinois preprint Ill(Th)-75-32 (1975), unpublished;
G. Sterman and S. Weinberg, Phys. Rev. Lett. 39 (1973) 1436.
[3] J. Ellis, M.K. Gaillard and G. Ross, Nucl. Phys. B111 (1976) 253.
[4] H. Fritzsch, M. Gell-Mann and H. Leutwyler, Phys. Lett. 47B (1973) 365;
D.J. Gross and F. Wilczek, Phys. Rev. D8 (1973) 3497;
S. Weinberg, Phys. Rev.Lett. 31 (1973) 31.
[5] C.H. Llewellyn Smith, Schladming Lectures 1978, Oxford preprint, unpublished, and references therein.
[6] Ch. Berger et al., Phys. Lett. 78B (1978) 176.
[7] F. Steiner, DESY preprint 78/59 (October 1978).
[8] S. Brandt et al., Phys. Lett. 12 (1964) 57;
S. Brandt and H. Dahmen, Siegen preprint SI 78-8;
E. Fahri, Phys. Rev. Lett. 39 (1977) 1587.
[9] A. De Rujula et al., Nucl. Phys. B138 (1978) 387.
[10] C.L. Basham, L.S. Brown, S.D. Ellis and S.T. Love, Seattle preprint RLO-1388-76 (Sept. 1978).
[11] B.L. Ioffe, Phys. Lett. 78B (1978) 277.
[12] A. Ali, J.G. Körner, G. Kramer and J. Willrodt, DESY preprint 78/47 (September, 1978).
[13] R.P. Feynman, Photon–hadron interactions (Benjamin, 1973).